Electronic supplementary information for

Biomimetic monolayer-protected gold nanoparticles for immunorecognition

Kellen M. Harkness, Brian N. Turner, Amanda C. Agrawal, Yibin Zhang, John A. McLean and David E. Cliffel*

I. Biomimicry of native antigens on AuNPs *in vitro*

Materials

$HAuCl_4 \cdot 3H_2O$ was synthesized according to standard methods[1] from electrochemically purified Canadian gold maple leaf coins (99.99%). Reagent and optima grade solvents, *N*-2-mercaptopropionylglycine (tiopronin), bovine serum albumin (fraction V, 96%), sodium borohydride, thioanisole, and anisole were purchased from Sigma-Aldrich. Common laboratory salts and concentrated ammonium hydroxide were reagent grade and purchased from Fisher Scientific. Concentrated sulphuric acid was purchased from EMD. Absolute ethanol was purchased from Pharmco-AAPER. Hydrogen peroxide (30% v/v) was purchased from Acros. Peptide synthesis materials (Fmoc- and side-chain-protected amino acids, coupling reagents, and resins) were obtained from the research group of Prof. David Wright (Vanderbilt University). Deionized water (18 MΩ) was obtained from a U.S. Filter Modulab water system with a 0.2 µm external filter or from a Barnstead NANOpure Diamond water purification system. Dry nitrogen is provided in house. Monoclonal antibody 1214, 1129, Palivizumab, and human respiratory syncytial virus were obtained from the research group of Prof. James Crowe, Jr. (Vanderbilt University). Work areas that contained HRSV were cleaned thoroughly with 70% isopropyl alcohol solution. Amicon Ultra molecular weight cut-off centrifuge tubes were obtained from the Molecular Biology Core Facility at Vanderbilt University. Snakeskin pleated dialysis tubing (10,000 MWCO) was purchased from Thermo Scientific. Deuterated solvents (99.9% D) were purchased from Cambridge Isotope Laboratories.

Peptide synthesis

Most peptides were synthesized by standard solid phase Fmoc procedures using an Apex automated peptide synthesizer (AAPPTec, Louisville, KY, USA). The peptides were cleaved from the resin and the side-chains deprotected using Reagent R (90% trifluoroacetic acid, 5% thioanisole, 3% ethanedithiol, 2% anisole). Following extraction in cold diethyl ether with cold centrifugation (0 °C), cleaved peptides were further purified using semi-preparative high-performance liquid chromatography (Waters Corp., Milford, MA, USA) with a reverse phase column in a continuous gradient of water:acetonitrile following injection in water/acetonitrile/dilute ammonium hydroxide. Samples were collected with a manually-operated fraction collector (Waters). *Note: ammonium hydroxide must be used sparingly, < 100 mM, to avoid damaging the column or corroding the pumping lines*. Following lyophilization, peptides were diluted in 20% acetonitrile and water, occasionally with the addition of ammonium hydroxide to increase solubility, and characterized by matrix-assisted laser desorption/ionization-time of flight-mass spectrometry (Voyager DE-STR, Applied Biosystems) with an α-cyano-4-hydroxycinnamic acid matrix. Some peptides were purified by size exclusion chromatography instead of semi-preparative HPLC.

ELISA stepwise linear epitope mapping of the full-length HRSV F antigenic site A

Linear fragments and full length linear peptides of antigenic site A were evaluated for their ability to bind Palivizumab in a peptide ELISA assay using maleimide coated well plates. The design of the peptides has been improved by amidation of the C terminus, and acylation of the N terminus to better represent the fact that the antigenic site A is an internal sequence. Serine-glycine-serine-glycine spacers were used instead of PEG-6 for improved synthetic yield, solubility, and ease of purification. The following synthetic peptides were evaluated by the assay:

Electronic Supplementary Material (ESI) for Nanoscale

Biomimetic self-assembled monolayers on gold nanoparticles for immunorecognition

Kellen M. Harkness, Brian N. Turner, Amanda C. Agrawal, Yibin Zhang, John A. McLean and David E. Cliffel*

Table S1 Peptides from the HRSV fusion protein antigenic site A which were evaluated against Palivizumab in an ELISA assay.Spaces allow for easy visualization of the stepwise differences between peptides. The amino acid numbering sequence for HRSV F protein is displayed in the top row. "Linker" indicates the cysteine terminus with an inert SGSG sequence added for peptide immobilization and projection. Residues known to bind to Motivizumab[2] are indicated in bold red type.

Designation	Linker	-	255	-	-	-	-	260	-	-	-	-	265	-	-	-	-	270	-	-	-	-	275	-	-	Linker
A	CSGSG	N	S	E	L	L	S	L	I	**N**	D	M	P	I	T	**N**	**D**	Q	K	K	L	M	**S**	N	N	
B		N	S	E	L	L	S	L	I	**N**	D	M	P	I	T	**N**	**D**	Q	K	K	L	M	**S**	N	N	GSGSC
1	CSGSG	N	S	E	L	L	S	L	I	**N**	D															
2	CSGSG		S	E	L	L	S	L	I	**N**	D	M														
3	CSGSG			E	L	L	S	L	I	**N**	D	M	P													
4	CSGSG				L	L	S	L	I	**N**	D	M	P	I												
5	CSGSG					L	S	L	I	**N**	D	M	P	I	T											
6	CSGSG						S	L	I	**N**	D	M	P	I	T	**N**										
7	CSGSG							L	I	**N**	D	M	P	I	T	**N**	**D**									
8	CSGSG								I	**N**	D	M	P	I	T	**N**	**D**	Q								
9	CSGSG									**N**	D	M	P	I	T	**N**	**D**	Q	K							
10	CSGSG										D	M	P	I	T	**N**	**D**	Q	K	K						
11	CSGSG											M	P	I	T	**N**	**D**	Q	K	K	L					
12	CSGSG												P	I	T	**N**	**D**	Q	K	K	L	M				
13	CSGSG													I	T	**N**	**D**	Q	K	K	L	M	**S**			
14	CSGSG														T	**N**	**D**	Q	K	K	L	M	**S**	N		
15	CSGSG															**N**	**D**	Q	K	K	L	M	**S**	N	N	
1b		N	S	E	L	L	S	L	I	**N**	D															GSGSC
2b			S	E	L	L	S	L	I	**N**	D	M															GSGSC
3b				E	L	L	S	L	I	**N**	D	M	P														GSGSC
4b					L	L	S	L	I	**N**	D	M	P	I													GSGSC
5b						L	S	L	I	**N**	D	M	P	I	T												GSGSC
6b							S	L	I	**N**	D	M	P	I	T	**N**											GSGSC
7b								L	I	**N**	D	M	P	I	T	**N**	**D**										GSGSC

Peptide ELISA step-wise linear epitope mapping

Peptides were evaluated in an ELISA assay at various concentrations of peptide, primary antibody (PZ), and labeled secondary antibody and with different wash solutions and development conditions until optimum conditions were obtained for the sequence A. These optimum conditions were determined to be 50 µg/mL peptide in PBS with 10mM EDTA, 5 µg/mL PZ in wash buffer, goat-anti-human diluted 1:5000 in wash buffer, and 10 minutes of developing time with TMB substrate followed by quenching with 1N H_2SO_4. The results of this assay are presented in Figure S1.

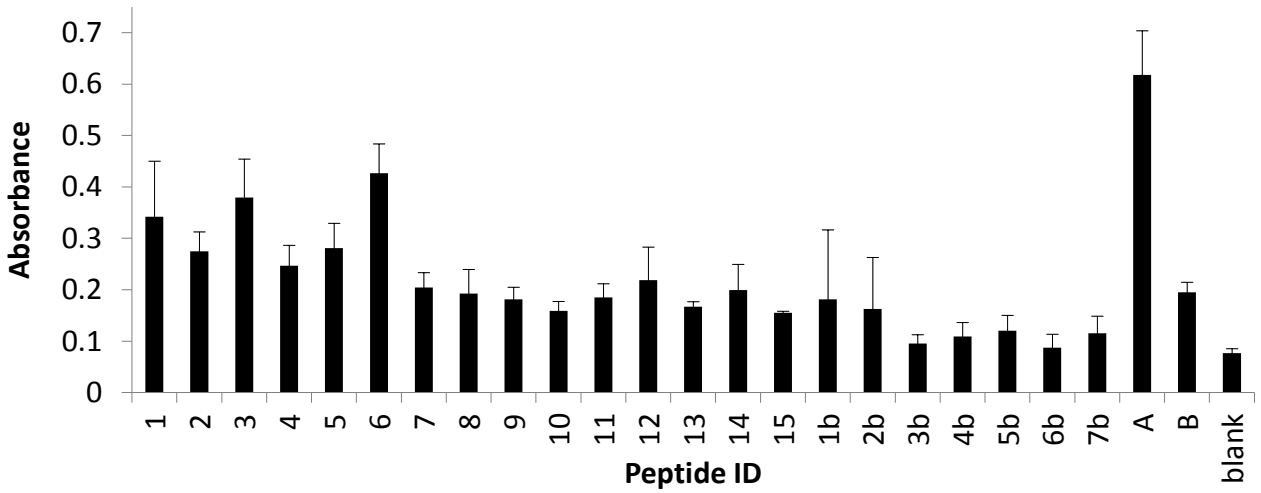

Figure S1 Results of the optimized peptide ELISA.The peptide IDs are listed in Table S1. Multiple null/alternate hypothesis pairs were evaluated from the ELISA data using Student's t-tests at a 95% confidence interval, assuming unequal variances, and a two-tailed distribution. The results are displayed in Table 5. Analysis of the true hypotheses allowed conclusions about which parts of the full peptide sequence A are important to the binding of PZ to HRSV F to be drawn.

Biomimetic self-assembled monolayers on gold nanoparticles for immunorecognition

Kellen M. Harkness, Brian N. Turner, Amanda C. Agrawal, Yibin Zhang, John A. McLean and David E. Cliffel*

Peptide A, a representation of the full region, binds PZ stronger than any of the peptide fragments. The same sequence presented in the reverse direction, peptide B, binds as effectively as sequences from peptides 7-15. Four out of six peptides (2, 3, 5, and 6) are significantly more active towards PZ than peptides oriented in the same direction but missing amino acids earlier in the chain (peptides 7 through 15). Furthermore, the pooled results of peptides 1-6 are significantly more active towards PZ than 7-15. Comparing segments from peptides 1-6 and 7-15 to the reversed sequence peptides 1b-7b, and the full length peptides A and B, it becomes clear that the orientation in which the peptides are displayed to PZ has a dramatic effect on binding affinity.

In conclusion, the most important observations to be made are that the full length epitope with the linker at the C terminus (B) shows little binding activity in ELISA (A = 0.195 ± 0.019), while the full length epitope with the linker at the N terminus (A) shows significant binding (0.618 ± 0.086). The difference in binding was attributed to a directionally dependent misalignment in the case of peptide B, as demonstrated in Figure S2.

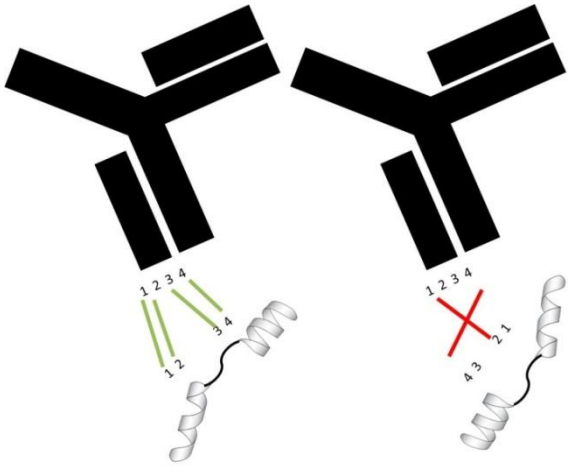

Figure S2 A conceptual interpretation of PZ approaching the synthetic peptide epitope in forward (left) and reverse (right) presentations. The illustrated concept might explain why PZ has such a strong preference for peptide A over peptide B.

QCM immunosensor construction and detection of HRSV

The assembly of the HRSV immunosensor on a QCM chip (Figure S3) was achieved as follows. A stable frequency baseline was collected while phosphate-buffered saline (PBS) was pumped through the flow cell with a peristaltic pump. Protein G (200 µg/mL) was pumped through the flow cell until saturation level was reached as indicated by a level frequency reading, at which point the solution was switched back to PBS. In the same manner, BSA (1 mg/mL) was then flowed, followed by Palivizumab (40 µg/mL). HRSV, diluted in PBS from growth medium to the desired concentration, was then flowed for a period of about 10 minutes. All solutions were in PBS and flowed at 20 µL/min. At the conclusion of each experiment all lines and flow cells were purged with 20% bleach solution to decontaminate. The sensor construction and subsequent detection of HRSV from cultured growth medium diluted in PBS is displayed in Figure S4.

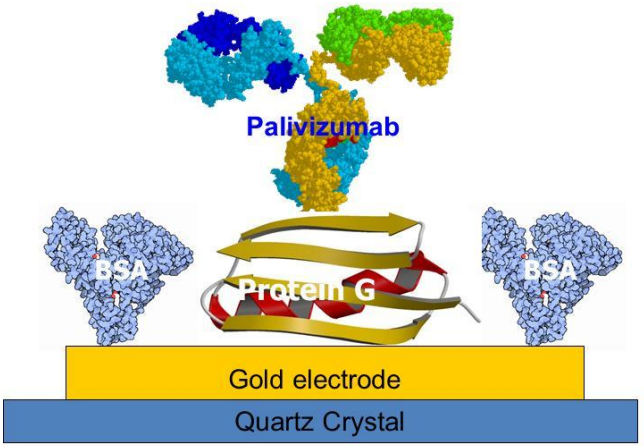

Figure S3 Cartoon schematic of the QCM based immunosensor for HRSV detection. Gold electrodes wrapped about piezoelectric quartz are functionalized with Protein G, which binds PZ in an orientation amenable to HRSV detection. BSA is used to fill in bare gold spaces left after adsorption of Protein G.

Biomimetic self-assembled monolayers on gold nanoparticles for immunorecognition

Kellen M. Harkness, Brian N. Turner, Amanda C. Agrawal, Yibin Zhang, John A. McLean and David E. Cliffel*

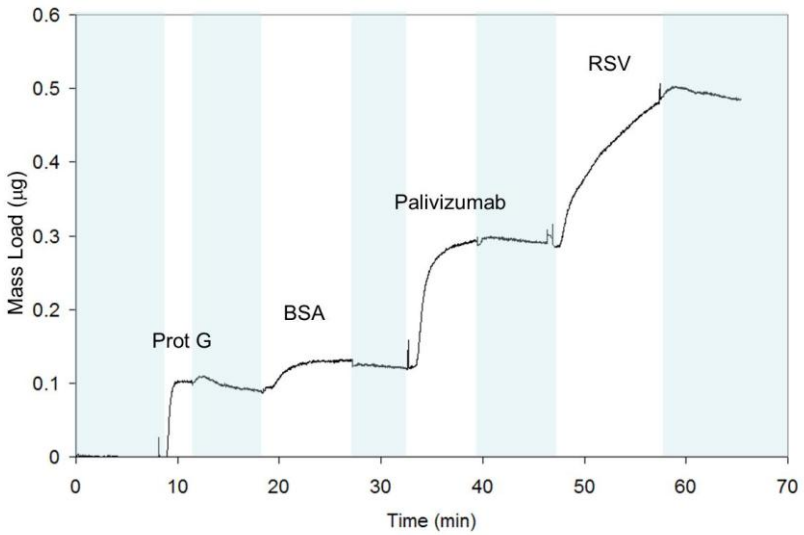

Figure S4 Detection of HRSV with the QCM-PZ immunosensor.Light blue indicates that PBS is being flowed without any analyte. "Prot G" indicates that Protein G (200 µg/mL) is flowed through the cell for the time duration designate in white, giving a total immobilized protein mass of 99 ng on the gold electrode surface. BSA (1 mg/mL) gave a mass of 35 ng, Palivizumab (40 µg/mL) gave a mass of 229 ng, and RSV (8 x 10^5 PFU/mL) yielded a detected viral mass of 210 ng. All solutions were in PBS and flowed at a rate of 20 µL/min.

Experiments to evaluate the specificity of the sensor are displayed in Figure S5. These experiments involved the replacement of the antibody and antigen to investigate the potential for false positives caused by non-specific binding. Anti-HA and anti-PA were compared to PZ for detection of HRSV and HRSV growth medium. Human metapneumovirus (HMPV), a close relative of HRSV, were compared to HRSV for detection by PZ. All detection steps were run for 10 minutes.

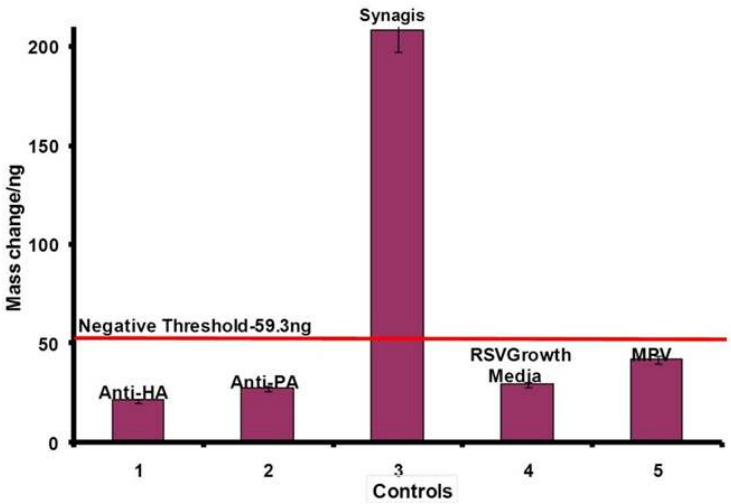

Figure S5 Detection and control experiments for the QCM immunonosensor. Experiments 1 and 2 are sensors detecting HRSV with anti-HA (mouse monoclonal 12CA3) and anti-PA (mouse monoclonal anti-PA83 from Alpha Diagnostics) replacing PZ, respectively. Experiment 3 is the detection experiment with HRSV and PZ (Synagis). Experiments 4 and 5 use the PZ immunosensor, but RSV growth medium and HMPV respectively are substituted for HRSV during the detection step.

The results from the HRSV growth medium are used as a negative background because it is present in the positive HRSV sample. A negative background was therefore determined as the signal of HRSV growth medium plus three standard deviations, which is 59.3 ng. Anything below this was determined to be a negative result for detection. Neither of the control antibodies provided significant signal when compared to PZ and to the negative threshold, indicating that HRSV is not significantly binding to other proteins in the sensing layer. Also, none of the other antigens provided a significant signal. The lack of HRSV growth media binding would indicate that the signal is not from contaminants in the HRSV sample that originate from the viral culture. The lack of HMPV binding suggests that the interaction between the Fab region of PZ and the antigenic surface protein of HRSV, in this case F, is of a nature dependent upon the specific primary and secondary structure of the HRSV F protein.

Biomimetic self-assembled monolayers on gold nanoparticles for immunorecognition

Kellen M. Harkness, Brian N. Turner, Amanda C. Agrawal, Yibin Zhang, John A. McLean and David E. Cliffel*

Synthesis of tiopronin-protected AuNPs

Tiopronin-protected AuNPs were synthesized as previously described.[3] Three syntheses were performed using varying gold:ligand molar ratios. $HAuCl_4 \bullet 3H_2O$ was dissolved in 6:1 methanol:acetic acid (~10 mg/mL) and chilled in an ice bath for 30 minutes. Tiopronin was then added to the solution, forming a ruby-red colour. Sodium borohydride (10:1 reductant:gold molar ratio) in approximately 10 mL water was then added to the mixture, producing a black solution of nanoparticles. The solution was stirred overnight. ^{1}H NMR (D_2O): δ 4.00 ppm (s, 2 H, CH_2) 3.76 ppm (s, 1 H, CH), 1.66 (s, 3 H, CH_3). TEM: average particle diameter of 2.2 ± 0.6 nm. UV/Visible spectroscopy: no surface plasmon resonance band observable.

- Synthesis 1: a ligand:gold molar ratio of 3.5:1 was used. The resulting AuNPs were cleaned by the following method. The solvent was removed via rotary evaporation, and the resulting precipitate/viscous acetic acid solution was redissolved in water. The pH was adjusted to 1 with concentrated hydrochloric acid and placed in dialysis tubing (cellulose ester, MWCO = 10 kDa). The dialysis proceeded for 2 weeks, changing the water at least twice daily. TGA: 33 weight percent organic (tiopronin).
- Synthesis 2: a ligand:gold molar ratio of 3:1 was used. The resulting solution was centrifuged and the solvent decanted. The particles were then resuspended in methanol, and centrifuged a second time. TEM: average particle diameter of 1.8 ± 0.7 nm. TGA: 33 % by mass organic (tiopronin).
- Synthesis 3: a ligand:gold molar ratio of 0.5:1 was used. The resulting solution is centrifuged, and the solvent decanted. The particles were then resuspended in methanol, and centrifuged a second time. TEM: average particle diameter of 2.9 ± 0.8 nm.

Place exchange to form series 3 peptide-nanoparticle conjugates

Peptides listed in Table S2 were place exchanged successfully onto tiopronin protected gold nanoparticles. Tiopronin-protected AuNPs (20 mg) were dissolved in 2 mL DI water, and then 0.1 molar equivalents (with respect to bound tiopronin) of a peptide was dissolved in 3 mL of water. The solutions were combined and stirred for 72 hours. The resulting nanoparticle-peptide conjugate solutions were subsequently transferred to 10,000 MWCO centrifuge filters for centrifugation. The resulting clean solutions were analyzed by ^{1}H NMR to determine purity and exchange percentages. Drying of the solution was avoided in order to reduce particle agglomeration. Buffers were used during place exchange and purification was utilized if there was a solubility or stability problem. ^{1}H NMR yielded the ratio of peptide to tiopronin on the surface, as demonstrated in Figure S6.

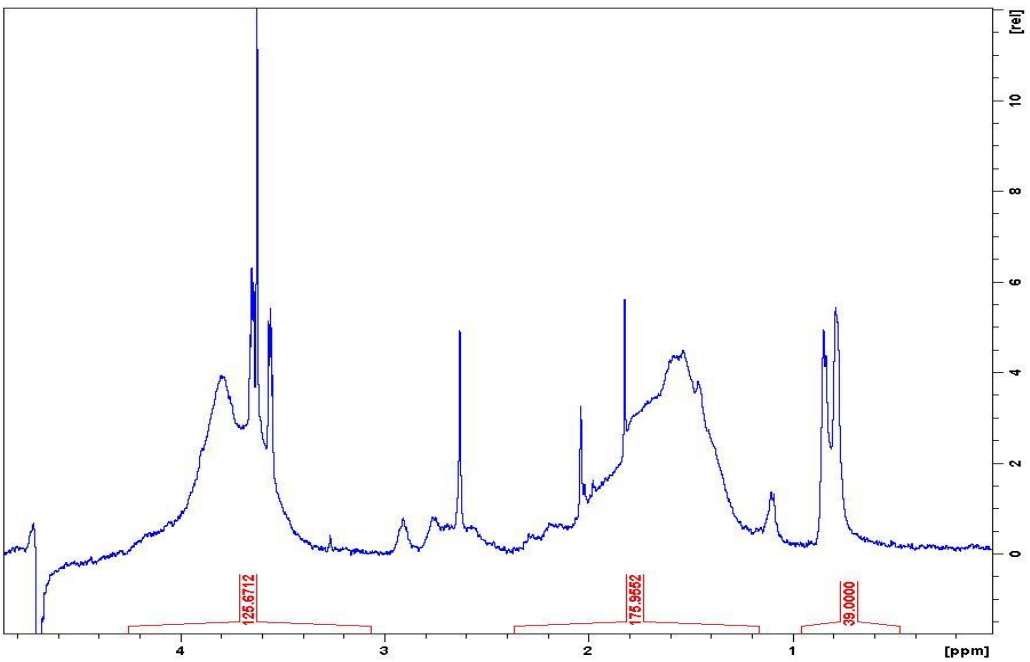

Figure S6 ^{1}H NMR, with double water-gate solvent suppression, of a peptide-nanoparticle conjugate, in this case $Au_{696}Tiopronin_{255}Peptide(3\text{-}F)_{10}$. The extent of peptide exchange is determined by integrating the peak at 0.8 ppm, which represents leucine, isoleucine, and valine methyl protons and comparing that to the peak at 1.5 ppm, which represents tiopronin methyl protons.

Adaptation of the QCM immunosensor to detect peptide presenting gold nanoparticles

The experimental design of the HRSV immunosensor was followed for sensor construction. In some cases the concentrations were adjusted to optimize sensitivity. Protein G was used at 50 µg/mL, BSA at 1mg/mL, and PZ at 10 µg/mL. Detection of the nanoparticle solution was achieved by diluting the water solution ≥4:1 in PBS to avoid inaccuracies in converting the frequency signal to bound mass caused by strong differences in solution conductivity and viscosity. The nanoparticle solution was then flowed through the cell as normal.

Biomimetic self-assembled monolayers on gold nanoparticles for immunorecognition

Kellen M. Harkness, Brian N. Turner, Amanda C. Agrawal, Yibin Zhang, John A. McLean and David E. Cliffel*

Table S2 Biomimetic tiopronin-protected AuNPs were utilized as a scaffold for the peptides shown. Each AuNP-epitope conjugate was tested for recognition by PZ. The peptides which were integrated into the monolayer (~5% final abundance) are indicated. Three different epitopes were selectively appended with cysteine (C, bold red type), SGSG, and/or PEG_6 linkers at the N- and/or C- termini in order to alter the projection of the epitope. The mimics which bound to PZ are given designations and discussed in the text.

Integrated peptide	d_{CORE} (nm)	Designation	Binding to Palivizumab
AcNH-**C**-SGSG-NSELLSLINDMPITNDQKKLMSNN-$CONH_2$	2.7	mimic A	strong
AcNH-**C**-PEG_6-NSELLSLINDMPITNDQKKLMSNN-$CONH_2$	1.8	mimic B	weak, non-specific
AcNH-NSELLSLINDMPITNDQKKLMSNN-PEG_6-**C**-$CONH_2$	1.8	-	none
AcNH-**C**-SGSG-NSELLSLINDMPITNDQKKLMSNN-GSGS-**C**-$CONH_2$	2.7	-	negligible
AcNH-**C**-PEG_6- NSELLSLINDMPITNDQKKLMSNN-PEG_6-**C**-$CONH_2$	1.8	-	none
H_2N-**C**-LSLINDMPITNDQKKLKKLMSNNVQ-COOH	2.2	-	none
H_2N-**C**-LSLINDMPITNDQKKLKKLMSNNVQ-**C**-COOH	2.2	-	none
AcNH-**C**-SGSG-SLINDMPITN	2.7	-	none
none	2.7	-	none
none	1.8	-	negligible

Study of mimic A-Palivizumab binding

In order to further characterize the affinity of mimic A for the PZ sensor, a concentration study was undertaken. Six concentrations of mimic A in PBS were evaluated for their bound mass and binding on rate. A Langmuirian binding model for an antigen and antibody was used in order to determine k_f, k_r, and K_a (Equation 1). The first case is appropriate for large antigens, such as virions, and the second case better describes smaller antigens (peptides, small proteins, nanoparticles).

$$\begin{aligned} Ab + Ag &\underset{k_r}{\overset{k_f}{\rightleftharpoons}} AbAg \quad K_a \\ 1/2\ Ab + Ag &\rightleftharpoons Ab_{1/2}Ag \end{aligned} \tag{1}$$

The data for mimic detection, along with data for the construction of the sensor layer for each experiment is summarized in Table S3.

Table S3 Summary of mimic A detection at various concentrations. The amount of Palivizumab and mimic A are provided, in addition to the mean number of AuNPs bound per antibody. None of the sample concentrations analyzed provided an empirical m_{max} in the time durations allowed due to continual and indefinite accumulation of material.

[Mimic A] (µg/mL)	**Palivizumab bound** (ng)	**Mimic A bound** (ng)	**Mimic A:PZ**
32.7	43	9.2	0.16
32.7	26	7.1	0.20
32.7	45	8.9	0.15
78.8	108	12	0.08
78.8	99	20	0.15
78.8	98	17	0.13
409	92	42	0.34
409	76	43	0.42
409	68	43	0.47
492	99	81	0.60
492	133	113	0.63

Normally, it is straightforward to determine equilibrium association (K_a) and dissociation (K_d) from *m* vs. *C* data, but in our case, the inability to determine saturation data renders this method unfeasible. Binding coefficients were instead determined from the maximum on rates at each concentration. Figure S7 illustrates the concentration dependence of the on rate.

Biomimetic self-assembled monolayers on gold nanoparticles for immunorecognition

Kellen M. Harkness, Brian N. Turner, Amanda C. Agrawal, Yibin Zhang, John A. McLean and David E. Cliffel*

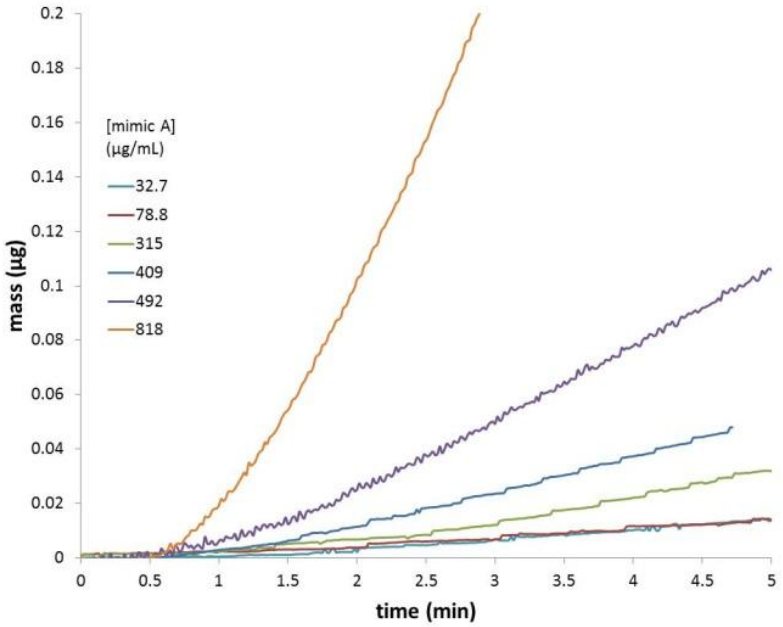

Figure S7 Representative QCM mass versus time curves at various concentrations of mimic A during the detection step.

For any binding model in Equation 1, the kinetics are characterized by:

$$ln\left(1-\frac{m_t}{m_{max}}\right) = -(\tau^{-1})t \quad (2)$$

where m_t is the bound mass at time t, m_{max} is the maximum mass that can bind to the sensor, the total quantity in the natural logarithm is the uncovered surface percentage and the fractional quantity is the surface coverage percentage at a given time, and τ is the time constant associated with a given concentration of antigen.[4,5] In order to determine m_{max} in the absence of data at saturation, a calculated value is used based on the average number of PZ molecules bound to the sensor. For a 2:1 binding model, which is expected for this system, m_{max} = 210 ng. This value of m_{max} provides better fits of data to theory than if individually calculated values for each sensor are used, probably because bound mass is not expected to track linearly with immobilized antibody due to the "hook effect."[6,7] The negative inverse time constant can be determined from the slope of the linear portion of a linear plot of Equation 1, in the form of the logarithmic quantity versus t, as illustrated in Figure S8 for one of the 409 µg/mL experiments.

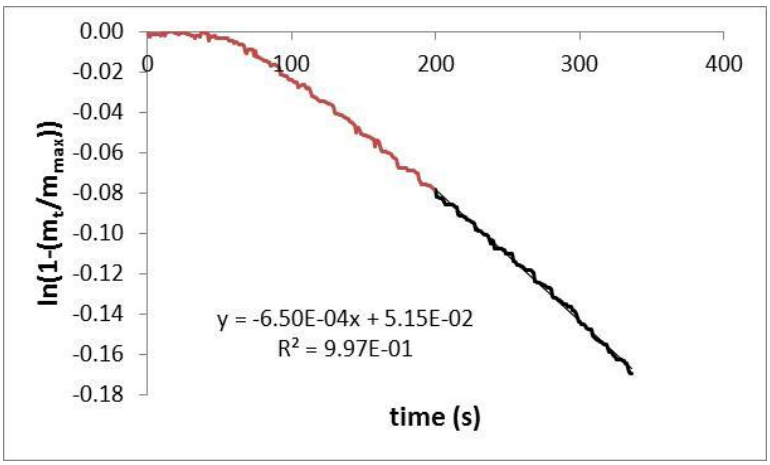

Figure S8 Plot to determine the time constant for mimic A binding to the Palivizumab sensor, τ, for a single experiment. For this 409 µg/mL experiment, $-\tau^{-1} = -6.50 \times 10^{-4}$ s^{-1}. The slope is only determined for the linear portion (black), where the binding rate has reached a maximum.

The binding coefficients are determined from the equation:

$$\tau^{-1} = k_f C + k_r \quad (3)$$

where C is the bulk concentration of mimic A. A linear plot of τ^{-1} versus C (in mol/L) yields a slope equal to k_f and a y-intercept equal to

Biomimetic self-assembled monolayers on gold nanoparticles for immunorecognition

Kellen M. Harkness, Brian N. Turner, Amanda C. Agrawal, Yibin Zhang, John A. McLean and David E. Cliffel*

k_r. For a 2:1 binding model, this yields the data shown in Figure S9.

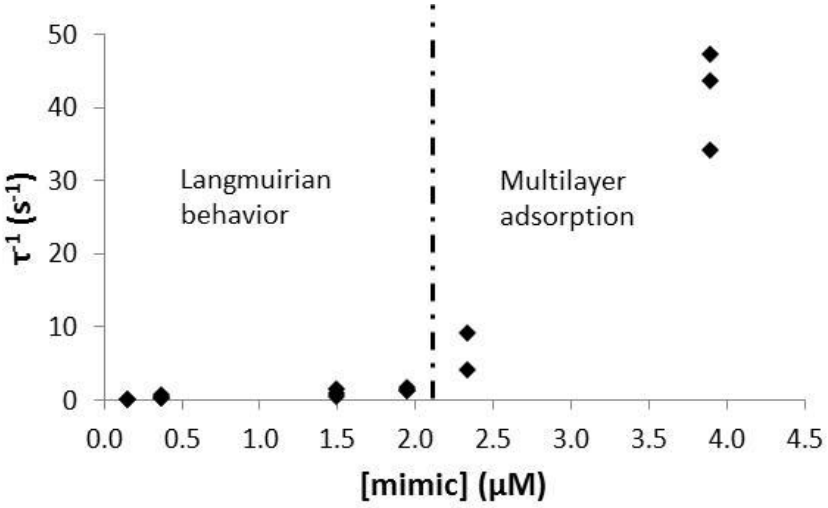

Figure S9 Plot of individual time constants determined for each concentration.Assuming a Langmuir isotherm, a linear plot will give a slope equal to k_f and a y-intercept equal to k_r. Above ~2 μM, linearity is broken, and the use of those data points to determine binding coefficients is not feasible. The most concentrated sample violates the 2:1 binding model.

From the data, it appears that the 2:1 Langmuir binding model is not valid for the entire process of mimic interacting with the sensor surface. A plausible explanation is found when the assumptions of the Langmuir isotherm are examined. The model assumes that surface coverage is restricted to a single monolayer and that interactions between adsorbates are negligible and all binding sites are equivalent. The equivalence of binding sites is violated to a certain extent, as there is no unidirectional relationship between the number of PZ molecules and the mass bound to the surface (see Table S2). Deviations were attributed to negative steric effects overtaking positive effects of increasing the total number of binding sites. Steric effects do not, however, explain the data in Figure S8. A more informed explanation was found by breaking the other two assumptions of the Langmuir isotherm. It was, therefore, assumed that the mimics could interact with each other, which would, in turn, lead to multilayer coverage. If true, one would expect that a 2:1 Langmuir model is insufficient. Plausibly, the system follows Langmuirian adsorption up to a certain concentration, which was defined as the point at which linearity is broken. If true, multilayer adsorption is catalyzed by surface immobilization of the first monolayer in a fashion similar to systems that follow a BET isotherm.[8] This theory also explains the reason why it was difficult to achieve saturation of the sensor (indicated by a plateau in the signal) after a somewhat lengthy period of time and use of a significant amount of material. Examining the four lowest concentrations, the plot in Figure S10 is produced.

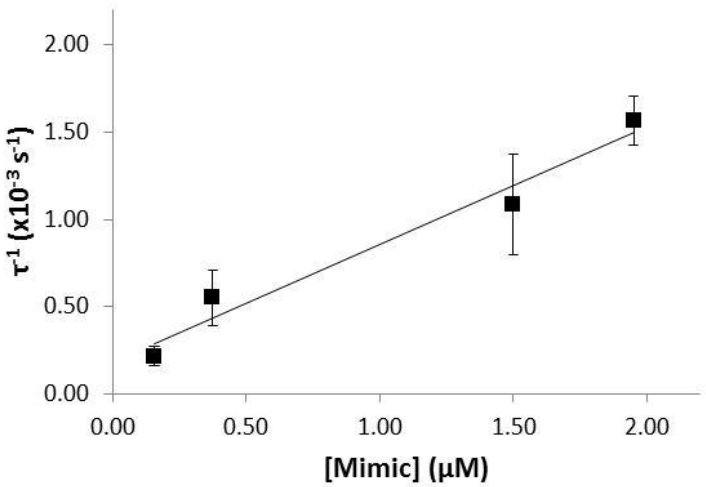

Figure S10 Plot to determine binding coefficients using the four lowest concentration samples.

If the four lowest concentrations are assumed to follow a Langmuirian isotherm, which they appear to, then, for a 2:1 binding model, it

Biomimetic self-assembled monolayers on gold nanoparticles for immunorecognition

Kellen M. Harkness, Brian N. Turner, Amanda C. Agrawal, Yibin Zhang, John A. McLean and David E. Cliffel*

is determined that $k_f = 6.74 \pm 0.88 \times 10^2$ M^{-1} s^{-1} and $k_r = 1.84 \pm 1.09 \times 10^{-4}$ s^{-1}. Therefore, when one considers that

$$K_a = \frac{[\mathrm{Ab_{1/2}Ag}]_s}{[Ab_{1/2}]_s[Ag]_{aq}} = \frac{k_f}{k_r} = \frac{1}{K_d} \quad (4)$$

then $K_a = 3.66 \pm 2.22 \times 10^6$ M^{-1}, and $K_d = 292 \pm 177$ nM.

II. *In vivo*: toxicity and biodistribution in murine models

Animal Models

Animals were female, 16-17 week old BALB/cAnNHsd mice weighing 20-22g and purchased from Harlan Sprague Dawley, Inc. The mice were housed under the supervision of full-time veterinarians and staff in a Vanderbilt Division of Animal Care (DAC) facility which was fully certified by the Association for the Assessment and Accreditation of Laboratory Animal Care (AAALAC). Animals were given *ad libitum* access to food and water and the animal room had a controlled photoperiod of 12 hr on, 12 hr off. All procedures were carried out in accordance with an Institutional Animal Care and Use Committees (IACUC) approved protocol. Mice were allowed one week to acclimate to their new housing prior to experimentation. Nanoparticles were dissolved in phosphate buffered saline (PBS) or sterile saline and injected subcutaneously. The two dosage concentrations used were 20 mg/kg (3 mg dissolved in 1.5 mL PBS) and 80 mg/kg (12 mg dissolved in 1.5 mL PBS). Each mouse was injected with a total volume of 200 µL nanoparticle solution. Baseline blood and urine samples were collected 1 week prior to injection (0 week) and at specific time points post-injection. Blood was drawn via submandibular bleeding[9] according to NIH bleeding guidelines for mL blood per kg body weight that can safely be taken per 2 weeks.[10] Urine was collected on cellophane sheets while avoiding fecal contamination as described in the literature.[11] Blood and urine were analyzed for gold content via inductively coupled plasma optical emission spectroscopy (ICP-OES) and red and white blood cell counts were determined by Coulter Counter or complete blood cell count to monitor immune response. The mice were euthanized 4 or 8 weeks post-injection via CO_2 asphyxiation and organs were harvested for histology and trace metal analysis.

Synthesis of GS AuNPs

Batch 1 glutathione (GSH)-protected gold nanoparticles (GS AuNPs) were synthesized in a 3:1 GSH/$HAuCl_4$•$3H_2O$ mole ratio in agreement with a modified Brust reaction.[3] Briefly, 1 g $HAuCl_4$•$3H_2O$ (2.54 mmol) and 2.34 g GSH (7.62 mmol) were codissolved in 100 mL 6:1 (v/v) methanol/acetic acid in a round bottom flask at 0°C. After 30 minutes of stirring, 0.95 g (10x mole excess of gold) $NaBH_4$ (25.40 mmol) was added quickly. The solvent was removed under vacuum and the nanoparticle slurry was dissolved in water and filtered through 0.2 micron syringe filters to remove particulates. The pH of the resulting dark brown nanoparticle solution was adjusted to ~2 with concentrated HCl and the solution was transferred to dialysis membrane tubing (Thermo Scientific, MWCO 10,000). The tubing was clamped on both ends and floated in 4L deionized water. Dialysis proceeded for 3 days with stirring, with water changes twice daily. The solution was then removed under vacuum and the resulting nanoparticles were characterized.

Batch 2 GS AuNPs were synthesized in a 1:1 GSH/$HAuCl_4$•$3H_2O$ mole ratio. Briefly, 1 g $HAuCl_4$•$3H_2O$ (2.54 mmol) and 0.945 g GSH (2.54 mmol) were codissolved in 100 mL methanol in a round bottom flask at 0°C. Immediately after GSH was dissolved, 0.95 g (10x mole excess of gold) $NaBH_4$ (25.40 mmol) was added quickly and the solution was allowed to stir for 30 minutes. MeOH was removed via centrifugation, and the particles were washed with MeOH and centrifuged 3x. After the final decantation the particles were dissolved in water and the solution was transferred to dialysis membrane tubing (Thermo Scientific, MWCO 10,000). The tubing was clamped on both ends and floated in 4L deionized water. Dialysis proceeded for 3 days with stirring, with water changes twice daily. The solution was then removed under vacuum and the resulting nanoparticles were characterized.

Electronic Supplementary Material (ESI) for Nanoscale

Biomimetic self-assembled monolayers on gold nanoparticles for immunorecognition

Kellen M. Harkness, Brian N. Turner, Amanda C. Agrawal, Yibin Zhang, John A. McLean and David E. Cliffel*

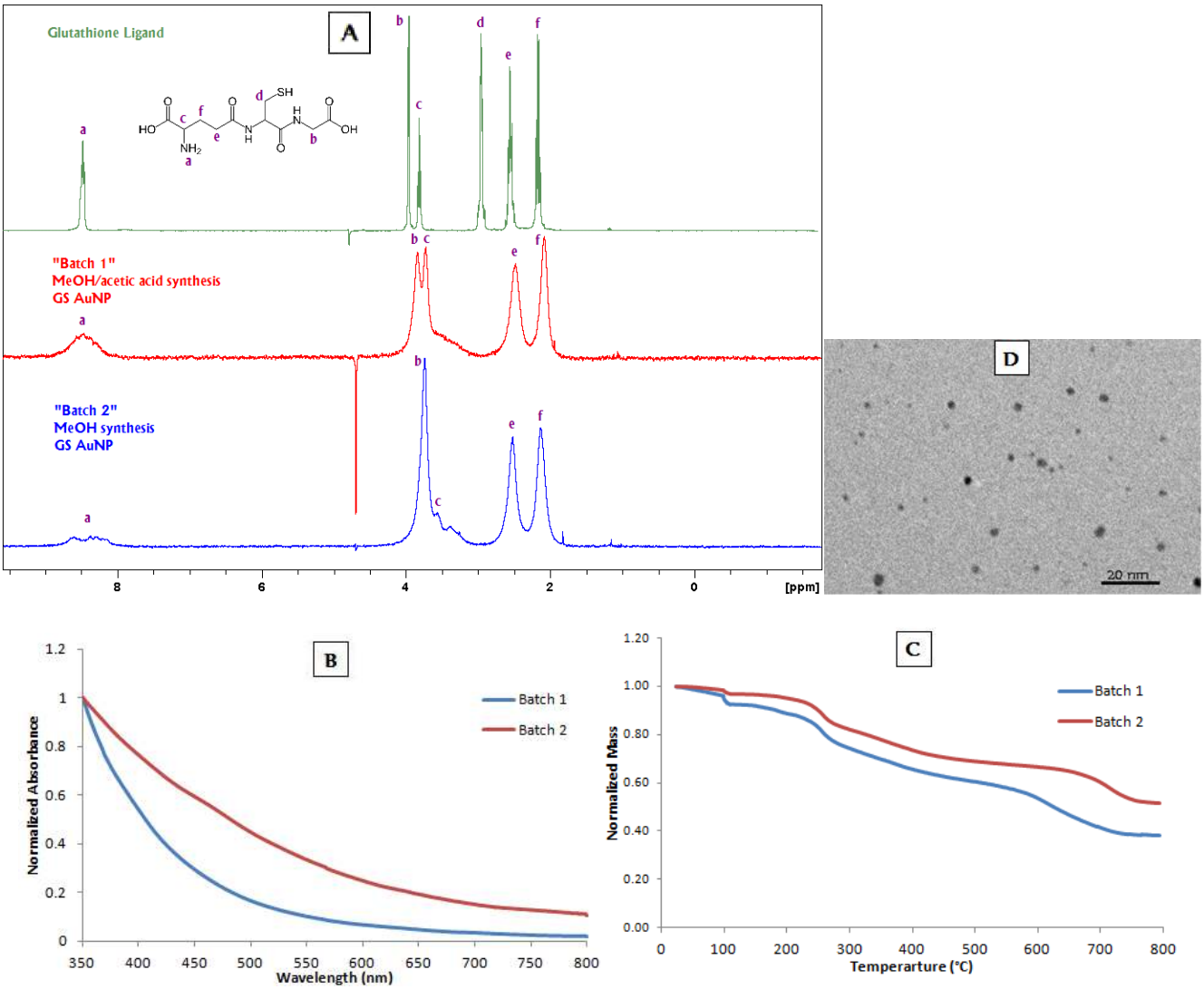

Figure S11 Characterization data for GS AuNPs. A) ^{1}H NMR spectra of GSH ligand (green), and Batch 1 GS AuNPs (red), and Batch 2 GS AuNPs (blue) showing characteristic peak broadening of nanoparticles; B) absence of a SP band at 520 nm in the UV-Vis spectrum indicates particles smaller than 5 nm in diameter; C) after subtracting water loss in the first weight loss step, the organic loss in the second step in TGA analysis accounts for 59% of the total mass in Batch 1, and 47% in Batch 2; D) representative TEM image showing an average particle diameter of 2.7 $\pm$ 0.7 nm.

Characterization data for Batch 1 and 2 GS AuNPs are shown in Figure S11. The peaks corresponding to the labeled protons in the glutathione structure are labeled in the ^{1}H NMR spectra of GSH (green), and in Batch 1 (red) and 2 (blue). At 8.2 ppm, the amide peak occurs and is present in all three spectra. Peaks b, d, e, and f correspond to methylenes while c is due to methine. The signal of the methylene closest to the thiol, peak d, is quenched in the AuNP spectra because of the proximity to the gold surface. The dissimilarity in magnitude of peaks b and c between Batch 1 and 2 is likely due to a variety of molecule orientations on the particle surface and differing packing densities. Another discrepancy between the particles born of the two syntheses can be found in TGA analysis. Batch 1 was determined to be 59% organic, while Batch 2 was only 47% organic. This may be explained by the fact that more ligand was available in the Batch 1 synthesis where a 3:1 ligand/gold ratio was employed compared to the 1:1 ratio used in Batch 2. The higher availability of GSH and perhaps the differing solvent systems allowed for more GSH to attach to the surface of Batch 1 nanoparticles. Despite the differences in the protecting layers, the average core sizes for the two batches were very similar, with 2.7±0.7 nm for Batch 1 and 2.7±0.6 nm for Batch 2.

Using NMR quantification (Figure S12), the ratio of ligand to peptide (L/P) on the nanoparticle surface was determined. The two peaks at 2.2 and 2.5 correspond to 4 methylene protons in glutathione, and the small peak around 0.8 ppm is from the 18 methyl protons from leucine and isoleucine in PA. In each spectrum, both of these peaks were integrated and the PA peak was calibrated to 18. The area of the two glutathione peaks was divided by 4 and the PA peak was divided by 18 to give an actual L/P. For loop PA-GS AuNPs, the ratio was found to be 32:1 GS/PA, while for linear PA-GS AuNPs, the ratio was 40:1 GS/PA.

Biomimetic self-assembled monolayers on gold nanoparticles for immunorecognition

Kellen M. Harkness, Brian N. Turner, Amanda C. Agrawal, Yibin Zhang, John A. McLean and David E. Cliffel*

ICP-OES Analysis

Samples were prepared as previously described[12] with the following modifications. For mice injected with Tio-PEG AuNPs, blood and urine samples were prepared by diluting 5 µL of the fluid in 1 mL aqua regia (3:1 hydrochloric acid/ nitric acid,). The blood samples were digested 24 hr in aqua regia before being further diluted in 9 mL 2% nitric acid (Optima grade, Fisher Scientific) while the 2% nitric acid was immediately added to the urine samples which required no digestion time. Organs were weighed, ground up, and dissolved in concentrated nitric acid for 48 h and heated to dryness. The organ residues were then reconstituted in 1 mL aqua regia where they were allowed to digest a further 24 h, and diluted in 9 mL 2% nitric acid. Blood and organ samples were centrifuged and decanted to remove remaining tissue and cells.

For mice injected with GS AuNPs and TioEG MPCs, trace metal grade nitric and hydrochloric acids were used to make aqua regia. Biological samples were diluted with 10% aqua regia in water. Measurements were made on a Perkin-Elmer ICP-OES Optima 700 DV using a Burgener Peek Mira Mist® nebulizer with an argon plasma flow of 15 L min^{-1}, nebulizer flow of 0.65 L min^{-1}, auxiliary flow of 0.2 L min^{-1}, pump flow of 1.6 mL min^{-1}, RF power at 1450 W, and a delay time of 30 s. Spectra were collected at a wavelength of 267.595 nm in triplicate, baseline-corrected, and averaged. Concentration values obtained for the organs are adjusted for weight and presented as concentration per gram organ.

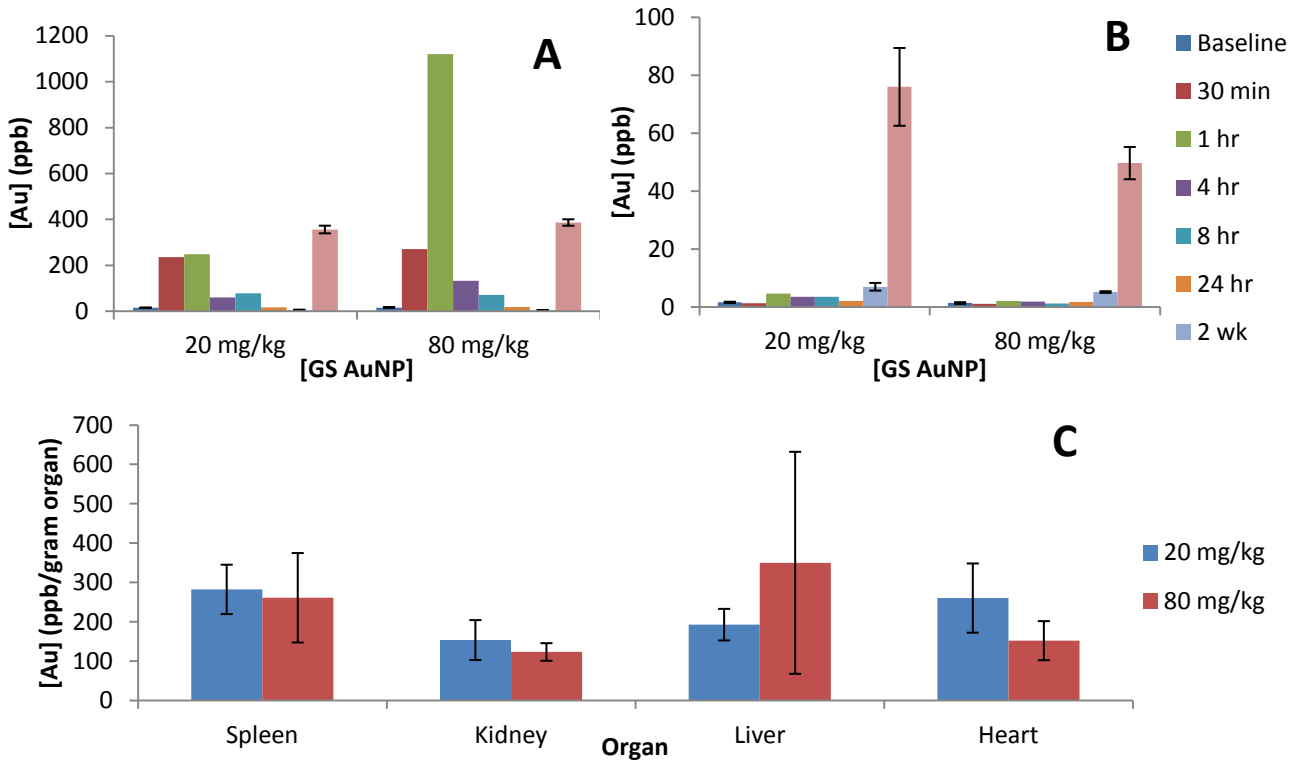

Figure S12 ICP-OES data for an initial 4-wk study of "Batch 1" GS AuNPs in a murine model. Graphs indicate Au concentration in urine (A) and blood (B) over time for two different dosages. Panel C represents Au concentrations in various organs at the conclusion of the study for the two dosages.

Electronic Supplementary Material (ESI) for Nanoscale
This journal is © The Royal Society of Chemistry 2012

Biomimetic self-assembled monolayers on gold nanoparticles for immunorecognition

Kellen M. Harkness, Brian N. Turner, Amanda C. Agrawal, Yibin Zhang, John A. McLean and David E. Cliffel*

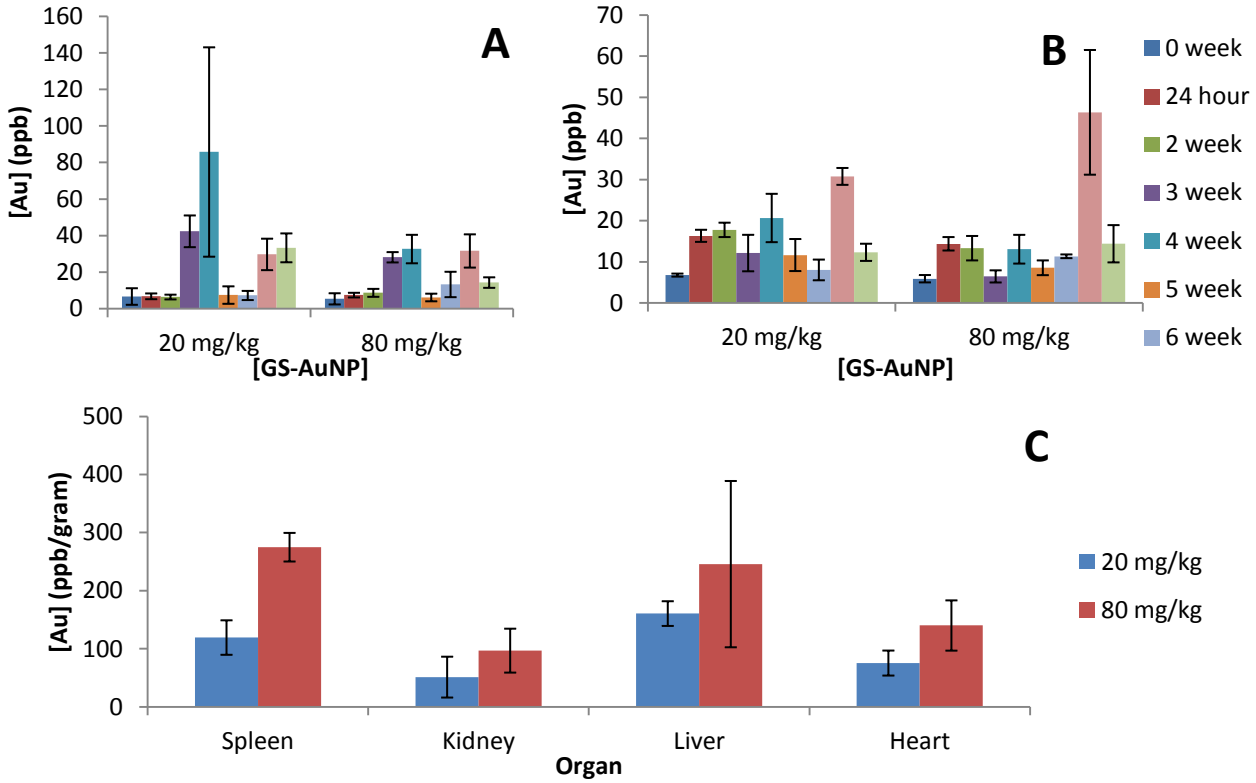

Figure S13 ICP-OES data for a second 8-wk study of "Batch 1" GS AuNPs in a murine model. Graphs indicate Au concentration in urine (A) and blood (B) over time for two different dosages. Panel C represents Au concentrations in various organs at the conclusion of the study for the two dosages.

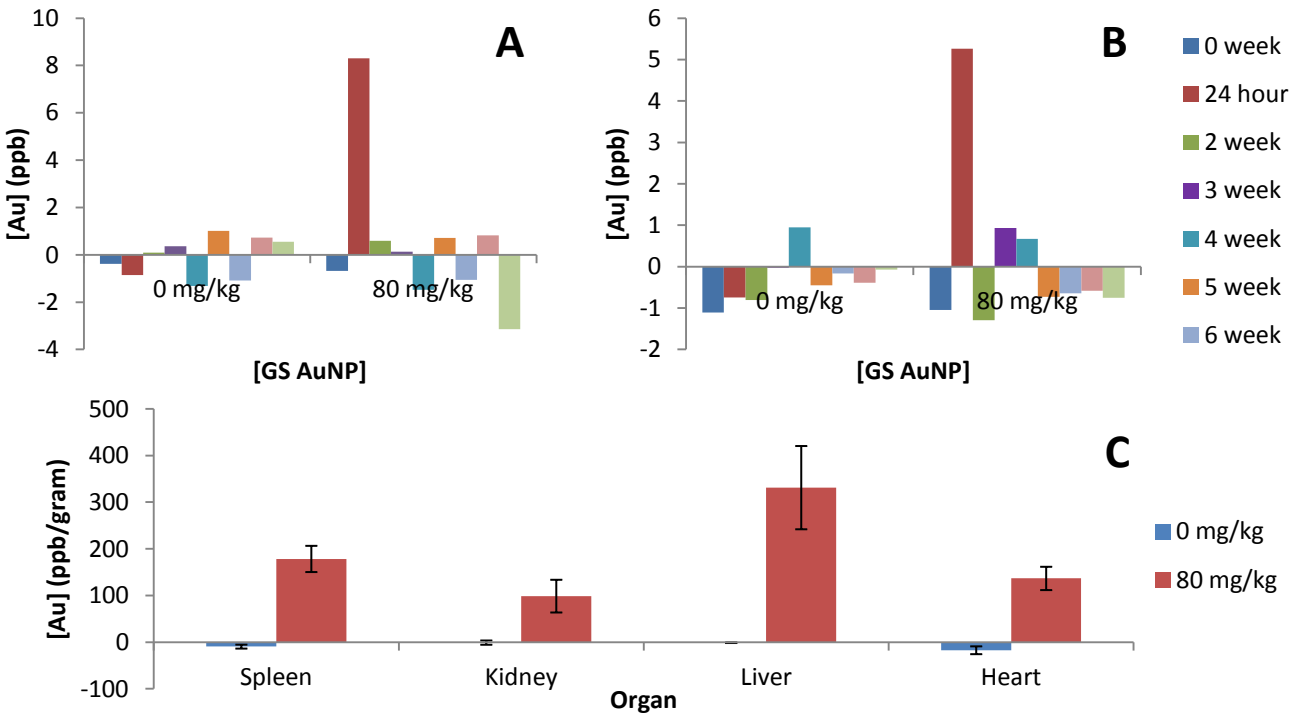

Figure S14 ICP-OES data for an 8-wk study of "Batch 2" GS AuNPs in a murine model. Graphs indicate Au concentration in urine (A) and blood (B) over time for the saline control (0 mg/kg) and 80 mg/kg dosage. Panel C represents Au concentrations in various organs at the conclusion of the study. Negative values are an artifact of baseline correction; noise in emission measurements (corresponding to ±1 ppm) may cause some values to appear negative.

Biomimetic self-assembled monolayers on gold nanoparticles for immunorecognition

Kellen M. Harkness, Brian N. Turner, Amanda C. Agrawal, Yibin Zhang, John A. McLean and David E. Cliffel*

Coulter Counter Analysis

Blood was analyzed on a Beckman Z1 Coulter Particle Counter. Samples were prepared for cell count analysis by diluting 40 µL whole blood in 20 mL Isoton® II Diluent (Beckman Coulter) for a 1:500 dilution of the blood specimen to be used as the WBC solution. The RBC solution was made by pipetting 200 µL of the WBC solution into 19.8 mL diluent to obtain a 1:50,000 dilution. The WBC solution received 8-10 drops of ZAP-OGLOBIN™ II lytic reagent (Beckman Coulter) and was agitated slowly. Red and white blood cell counts were then collected in triplicate and averaged.

Histology

Organs were excised shortly after euthanasia and sections of kidney were immediately fixed in 10% formalin, neutral buffered with 0.03% eosin (Sigma-Aldrich), and sent to Vanderbilt University Medical Center Immunohistochemistry Core Lab for hematoxylin and eosin (H&E) staining. The slides were interpreted by K. Salleng, D.V.M., Vanderbilt University Division of Animal Care.

References

1. G. Brauer, ed., *Handbook of preparative inorganic chemistry*, Academic Press, New York, 1965.
2. J. S. McLellan, M. Chen, A. Kim, Y. Yang, B. S. Graham and P. D. Kwong, *Nat. Struct. Mol. Biol.*, 2010, **17**, 248-250.
3. A. C. Templeton, S. Chen, S. M. Gross and R. W. Murray, *Langmuir*, 1999, **15**, 66-76.
4. Y. Ebara, K. Itakura and Y. Okahata, *Langmuir*, 1996, **12**, 5165-5170.
5. H. Ebato, C. A. Gentry, J. N. Herron, W. Mueller, Y. Okahata, H. Ringsdorf and P. A. Suci, *Anal. Chem.*, 1994, **66**, 1683-1689.
6. D. Rodbard, Y. Feldman, M. L. Jaffe and L. E. M. Miles, *Immunochem.*, 1978, **15**, 77-82.
7. R. G. Ryall, C. J. Story and D. R. Turner, *Anal. Biochem.*, 1982, **127**, 308-315.
8. I. A. Vinokurov and J. Kankare, *Langmuir*, 2002, **18**, 6789-6795.
9. W. T. Golde, P. Gollobin and L. L. Rodriguez, *Lab Anim.*, 2005, **34**, 39-43.
10. Guidelines for Survival Bleeding of Mice and Rats, http://oacu.od.nih.gov/ARAC/Bleeding.pdf.
11. B. T. Kurien and R. H. Scofield, *Lab. Anim.*, 1999, **33**, 83-86.
12. C. A. Simpson, B. J. Huffman, A. E. Gerdon and D. E. Cliffel, *Chem. Res. Toxicol.*, 2010, **23**, 1608-1616.